400–600 °C temperature ranges. In going from 800 to 1500 °C in N_2, a small amount of nitrogen is lost, while in going from 800 to 1600 °C, an even greater amount of nitrogen is lost. Schmidt et al. have shown that precursor-derived silicon nitride begins to decompose in 1 atm of helium at approximately 1000 °C with major decomposition beginning at 1500 °C.[41] Thus, the loss of nitrogen in the sample heated to 1500 °C in N_2 and the sample heated to 1600 °C in N_2 can be attributed to decomposition of silicon nitride. As is shown by the elemental analysis data obtained after heating to 1500 °C in argon, this loss of nitrogen is increased substantially when N_2 is excluded from the gas phase. This substantiates the solid-state NMR and IR data showing the reaction of silicon nitride and carbon to give silicon carbide and N_2.

The analytical data also show steady loss of hydrogen in heating PCS-Et to 500–800 °C. This is consistent with the gaseous analysis showing loss of hydrocarbons, ammonia, and amines over this temperature interval. In addition, molecular hydrogen may be produced; it was not specifically investigated. By 800 °C the amount of hydrogen left is less than 0.5%.

Conclusions

PCS-Et has been shown to decompose to either silicon nitride or silicon carbide, depending on the atmosphere used when heating above 800 °C. Heating PCS-Et to 500 °C results mostly in further cyclization and/or branching of the polymer with little decomposition of the hydrocarbon substituents. For a sample heated to 800 °C, FTIR and ^{29}Si MAS NMR reveal that the product contains amorphous silicon nitride and little silicon–carbon functionality. Elemental analysis shows the presence of carbon in the sample, and ^{13}C MAS NMR suggests that it is, at least in part, in the form of graphite. Heating the 800 °C product to 1500 °C in argon results in mostly β-SiC and carbon with some α-SiC, and heating to 1600 °C in N_2 results in mostly α-Si_3N_4 and carbon with a minor amount of β-SiC.

The most notable observation is the retention of the SiN_4 structural environment for Si throughout the conversion of the polymeric silazane to the amorphous ceramic product at 800 °C, albeit with the formation of a considerable amount of free carbon as a byproduct of hydrocarbon (or hydrocarbon radical) decomposition. This carbon byproduct is then available for reaction with the amorphous Si_3N_4, leading to the production of crystalline SiC observed on heating to 1500 °C. The loss of nitrogen that accompanies this latter process is inhibited by the presence of this gas in the pyrolysis environment, resulting in the formation of crystalline Si_3N_4 on heating to 1600 °C in 1 atm of N_2.

Acknowledgment. We thank Dr. Wayde Schmidt for his assistance with the high-temperature furnace runs, Dr. Frederick C. Sauls for his help in editing the manuscript, and Dr. Charles E. Bronnimann for the ^1H CRAMPS spectra. This work was supported by a NSF Materials Chemistry Initiative Grant (CHE-8706131) and the Colorado State University Regional NMR Center, funded by National Science Foundation Grant (CHE-8616437).

Synthesis of Amide- and Ester-Functionalized Zirconium Phosphonates

David A. Burwell and Mark E. Thompson*

Department of Chemistry, Princeton University, Princeton, New Jersey 08544

Received January 30, 1991. Revised Manuscript Received May 28, 1991

The syntheses of layered amide and ester derivatives of $Zr(O_3PCH_2CH_2COOH)_2$ are described. These new materials, $Zr(O_3PCH_2CH_2COXC_nH_{2n}H)_2$ (X = NH, n = 0–18; X = O, n = 2–6), are prepared via amine and alcohol intercalation reactions of layered $Zr(O_3PCH_2CH_2COCl)_2$. They are characterized by powder X-ray diffraction, IR, and ^{13}C CP MAS NMR spectroscopies as well as by thermogravimetric analysis. The interlayer separation in these materials is directly related to the length (n) of the amide or ester alkyl chain. For amides, the interlayer distance varies from 13.8 to 53 Å and is consistent with an angle of 59° between the the alkyl chain and the surface of the inorganic layer. The layered amide compounds have greater thermal and chemical stabilities than analogous compounds prepared by Brønsted acid/base reactions. A bridging ester derivative, $Zr(O_3PCH_2CH_2COOCH_2CH_2CH_2PO_3)$, has also been prepared by the reaction of $Zr(O_3PCH_2CH_2COCl)_2$ with $HSn(C_4H_9)_3$.

Introduction

The intercalation of organic molecules into layered inorganic compounds has been studied by a number groups over the past 25 years.[1] In this reaction inorganic host layers separate to accommodate interaction with organic guest molecules. A fully intercalated material consists of regularly alternating organic and inorganic layers as shown schematically in Figure 1. Intercalation can significantly alter both the physical nature and chemical reactivity of a host. For example, intercalation has been used to modify a host's optical properties, superconducting critical temperature, and interlayer magnetic coupling.[1,2] Applications of intercalation compounds include materials design,[3] ion exchange,[4] and catalysis.[5] Some recent and very inter-

(1) *Intercalation Chemistry*; Whittingham, M. S., Jacobson, A. J., Eds.; Academic Press Inc.: New York, 1982.

(2) Schöllhorn, R. In *Inclusion Compounds*; Academic Press: London, 1984, and references therein. (b) Dresselhaus, M. S. *Mater. Sci. Eng., B1* 1988, 259–277 and references therein. (c) Formstone, C. A.; Fitzgerald, E. T.; O'Hare, D.; Cox, P. A.; Kurmoo, M.; Hodby, J. W.; Lillicrap, D.; Goss-Custard, M. *J. Chem. Soc., Chem. Commun.* 1990, 501–503.

(3) (a) Clearfield, A. In *Design of New Materials*; Cocke, D. L., Clearfield, A, Eds.; Plenum Press: New York, 1988. (b) Giannelis, E. P.; Mehrota, V.; Russell, M. W. *Mater. Res. Soc. Proc.* 1990, 180.

0897-4756/91/2803-0730$02.50/0

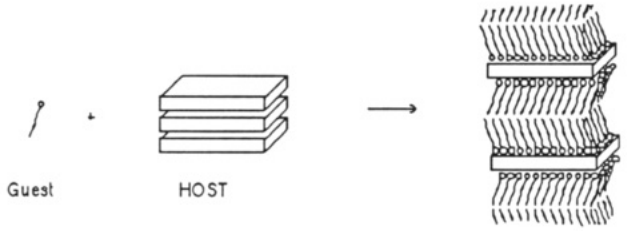

Figure 1. General intercalation reaction.

esting applications involve the use of these compounds to modify electrode surfaces,[6] prepare low-dimensional conducting polymers,[7] and assemble molecular multilayers at solid–liquid interfaces.[8]

The methods used to promote intercalation of organic guest molecules into inorganic hosts are very similar to those used to promote intercalation of inorganic ions (i.e., main-group and transition-metal ions and inorganic complexes, such as $FeCl_4^-$). Ion-exchange and acid/base reactions are those most commonly employed for preparing organic intercalation compounds (eqs 1 and 2, respectively,

$$G^+ + G^+_xHOST^{x-} \rightarrow G^+ + G^+_xHOST^{x-} \quad (1)$$

$$G + HOST^-H^+ \rightarrow GH^+HOST^- \quad (2)$$

$$G + HOST \rightarrow G^+_xHOST^{x-} \quad (3)$$

$$Zr(O_3POH)_2 + 2\overbrace{CH_2CH_2O} \rightarrow Zr(O_3POCH_2CH_2OH)_2 \quad (4)$$

where G is the organic guest molecule and HOST is the layered inorganic host). Although a Brønsted acid–base reaction is depicted in eq 2, Lewis acid/base interactions can be used as well. In the latter case, the guest is typically a Lewis base and the host layers contain Lewis acidic, coordinatively unsaturated metal atoms. Redox reactions, eq 3, are routinely used to prepare inorganic intercalation compounds, but are less common for organic compounds. Equation 4 shows a unique organic intercalation reaction of ethylene oxide with the Brønsted acidic host $Zr(O_3POH)_2 \cdot H_2O$ (α-ZrP).[9] This type of reaction is possible only for organic compounds and is one of the few examples of intercalation promoted by a simple organic reaction. While these methods have afforded a large number of interesting compounds, it is surprising that a wider range of reactions has not been employed to promote intercalation of organic guest molecules.

In 1978, Alberti et al. reported the synthesis of a new class of layered metal(IV) phosphate and phosphonate solids that contain both inorganic and organic groups.[10] These compounds have the general formula $M(O_3POR)_2$ and $M(O_3PR)_2$, respectively, and are prepared by treating a metal(IV) salt with H_2O_3POR or H_2O_3PR in H_2O. HF is added to slow the precipitation and produce reasonably crystalline materials. A broad range of tetravalent metal

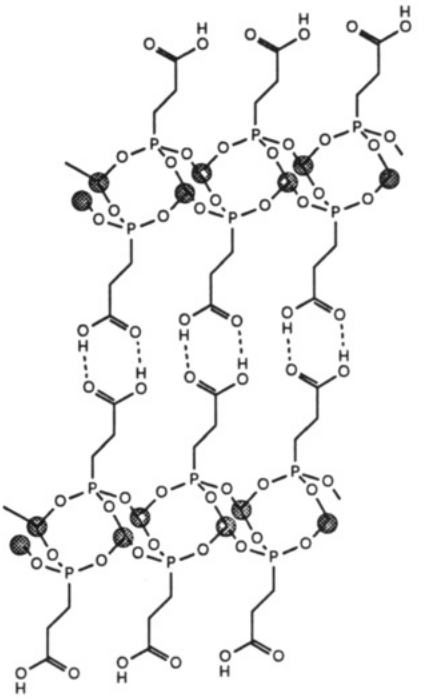

Figure 2. Schematic drawing of **1**.

phosphates and phosphonates were prepared in this way by Dines and co-workers in the early 1980s, including $Zr(O_3PC_6H_5)_2$ and $Zr(O_3P(CH_2)_nX)_2$ (n = 1–5; X = H, Cl, SH, SEt, OH, COOH, SO_3H, OC_6H_5).[11] Although zirconium phosphonates have been studied most extensively, isostructural complexes have also been made with the rest of the group 4 elements (i.e., Ti, Hf, Ce, Th). More recently, layered vanadium(IV) phosphonates,[12] divalent metal (Mg, Mn, Zn, Ca, Cd) phosphonates,[13] and trivalent metal (La, Sm, Ce, Fe) phosphonates[14] have been synthesized, and their intercalation chemistry has been investigated. Throughout all this work, the organic functionality of the phosphonates has been limited to groups that are stable in acidic aqueous or acidic aqueous/alcoholic media, such as alkyl, phenyl, COOH, SO_3H, SH, and OH. Excellent reviews on the structure, properties, and applications of layered phosphates and phosphonates have appeared in recent years.[4a,15]

The group 4 metal phosphates crystallize with layered structures similar to α-ZrP. Each layer consists of a plane of metal atoms linked together by phosphonate groups. The metal atoms are octahedrally coordinated by oxygen atoms, with the three oxygens of each phosphonate tet-

(4) (a) Alberti, G.; Constantino, U. In ref 1, Chapter 5. (b) Alberti, G.; Constantino, U.; Marmottini, F. In *Recent Developments in Ion Exchange*; Williams, P. A., Hudson, M. J., Eds.; Elsevier Applied Science: New York, 1987. (c) Clearfield, A. *Chem. Rev.* **1988**, *88*, 125–148.

(5) (a) Alberti, G.; Constantino, U. *J. Mol. Catal.* **1984**, *27*, 235–250. (b) Clearfield, A. *J. Mol. Catal.* **1984**, *27*, 251–262.

(6) (a) Li, Z.; Lai, C.; Mallouk, T. E. *Inorg. Chem.* **1989**, *28*, 178–182. (b) Rong, D.; Kim, Y. I.; Mallouk, T. E. *Inorg. Chem.* **1990**, *29*, 1531–1535.

(7) (a) Kanatzidis, M. G.; Wu, C.; Marcy, H. O.; DeGroot, D. C.; Kannewurf, C. R. *Chem. Mater.* **1990**, *2*, 222–224. (b) Kanatzidis, M. G.; Hubbard, M.; Tonge, L. M.; Marks, T. J.; Marcy, H. O.; Kannewurf, C. R. *Synth. Met.* **1989**, *28*, C89–C95.

(8) Lee, H.; Kepley, J.; Hong, H.; Mallouk, T. E. *J. Am. Chem. Soc.* **1988**, *110*, 618–620.

(9) Ortiz-Avila, C. Y.; Clearfield, A. *Inorg. Chem.* **1985**, *24*, 1773–1778.

(10) Alberti, G.; Constantino, U.; Allulli, S.; Tomassini, N. *J. Inorg. Nucl. Chem.* **1978**, *40*, 1113–1117.

(11) (a) Dines, M. B.; DiGiacomo, P. M. *Inorg. Chem.* **1981**, *20*, 92–97. (b) Dines, M. B.; Griffith, P. C. *Polyhedron* **1983**, *2*, 607–611. (c) Dines, M. B.; Griffith, P. C. *Inorg. Chem.* **1983**, *22*, 567–569. (d) Dines, M. B.; Cooksey, R. E.; Griffith, P. C.; Lane, R. H. *Inorg. Chem.* **1983**, *22*, 1004–1006.

(12) (a) Johnson, J. W.; Jacobson, A. J.; Brody, J. F.; Lewandowski, J. T. *Inorg. Chem.* **1984** *23*, 3842–3844. (b) Johnson, J. W.; Jacobson, A. J.; Butler, W. M.; Rosenthal, S. E.; Brody, J. F.; Lewandowski, J. T. *J. Am. Chem. Soc.* **1989**, *111*, 381–383. (c) Huan, G.; Jacobson, A. J.; Johnson, J. W.; Corcoran, E. W., Jr. *Chem. Mater.* **1990**, *2*, 91–93. (d) Johnson, J. W.; Brody, J. F.; Alexander, R. M.; Pilarski, B.; Katritzky, A. R. *Chem. Mater.* **1990**, *2*, 198–201.

(13) (a) Cao, G.; Lee, H.; Lynch, V. M.; Mallouk, T. E. *Inorg. Chem.* **1988**, *27*, 2781–2785. (b) Cao, G.; Lee, H.; Lynch, V. M.; Mallouk, T. E. *Solid State Ionics* **1988**, *26*, 63–69. (c) Ortiz-Avila, C. Y.; Rudolf, P. R.; Clearfield, A. *Inorg. Chem.* **1989**, *28*, 2137–2141.

(14) (a) Cao, G.; Lynch, V. M.; Swinnea, J. S.; Mallouk, T. E. *Inorg. Chem.* **1990**, *29*, 2112–2117. (b) Bujoli, B.; Palvadeau, P.; Rouxel, J. *Chem. Mater.* **1990**, *2*, 582–589.

(15) (a) Clearfield, A. *Comments Inorg. Chem.* **1990**, *10*, 89–128. (b) Alberti, G. In *Recent Developments in Ion Exchange*; Williams, P. A., Hudson, M. J., Eds.; Elsevier Applied Science: New York, 1987.

rahedron bound to three different metal atoms. This arrangement forces the organic groups to lie above and below the inorganic layer. In contrast to α-ZrP, which contains no *interlayer* hydrogen bonds,[16] interlayer hydrogen bonding is observed in some tetravalent metal phosphonates. For example, the pendant acid groups in $Zr(O_3PCH_2CH_2COOH)_2$ associate in interlayer dimer-type interactions, as depicted schematically in Figure 2.[17] Like α-ZrP, $Zr(O_3PCH_2CH_2COOH)_2$ readily intercalates *n*-alkylamines in a Brønsted acid/base reaction to give $Zr(O_3PCH_2CH_2COO^-RNH_3^+)_2$, despite the additional interlayer hydrogen bonding.[4a,18] This reaction demonstrates that an organic acid can promote intercalation of polar organic molecules, resulting in compounds with structures and chemical and thermal stabilities similar to the α-ZrP intercalation compounds.

The synthesis of layered metal phosphates and phosphonates with different reactive groups on the surfaces of the host lamellae introduces the possibility of promoting intercalation by reactions other than simple acid/base, ion exchange, or redox. We recently reported one such reaction in the synthesis of the Lewis acidic layered solid $Zr(O_3PCH_2CH_2COCl)_2$, **3**, from $Zr(O_3PCH_2CH_2COOH)_2$, **1**.[19] Here we investigate the possibility of promoting intercalation via organic reactions of **3**. The syntheses of previously unobtainable layered zirconium(IV) phosphonates containing amide and ester linkages are reported. These new derivatives retain the layered structure of **1** and are in many ways similar to the materials prepared by Brønsted acid/base intercalation. However, the covalent nature of the host–guest interaction gives this new class of organic intercalation compounds enhanced chemical and thermal stability.

Experimental Section

General Methods. Room-temperature ^{13}C and ^{31}P solid-state NMR spectra were recorded on a JEOL 270-MHz spectrometer (67.9 and 109 MHz for ^{13}C and ^{31}P, respectively) equipped with either a 7-mm magic angle spinning (MAS) probe from Doty Scientific or a 7.5-mm MAS probe from Chemagnetics, Inc. High-power ^1H decoupling, cross polarization (CP), and MAS were employed for all ^{13}C spectra. A 50-kHz field strength was used for both ^1H decoupling and cross polarization; spinning speeds were 3.5–4.0 kHz. ^{13}C signals were referenced to TMS (downfield shifts positive) by using adamantane as a secondary external reference. High-power ^1H decoupling and MAS were employed for ^{31}P spectra. ^{31}P signals were externally referenced to 85 wt % H_3PO_4 (downfield shifts positive).

FTIR spectra were obtained on a Nicolet 730 FT-IR spectrometer at a resolution of 4 cm^{-1}. A Du Pont Instruments Thermogravimetric Analyzer 951 and Thermal Analyst 2000 Workstation were used to obtain TGA thermograms. Thermograms were run in an air atmosphere from room temperature to 1150 °C at a scan rate of 10 °C/min.

Powder X-ray diffraction (XRD) patterns were obtained by using either a Scintag PAD-V or a Philips Electronics Instruments diffractometer (both Cu Kα radiation). XRD analyses were usually conducted with powders that were preferentially aligned on a quartz single crystal or microscope slide. When obtained in this manner, the diffraction patterns show several orders of 00*l* reflections, allowing for easy calculation of the interlayer spacings (*c*-axis repeat distance). The calculated standard deviations for the interlayer spacings were less thn 0.7 Å.

Materials. Except where noted, all starting materials were purchased from Aldrich Chemical Co. and were used as received.

Synthesis of $Zr(O_3PCH_2CH_2COOH)_2$, 1. **1** was prepared according to the literature procedure of Dines and DiGiacomo.[11a] **1**: IR (KBr) 3600–2500 (s, v br), 1700 (vs), 1432 (s), 1410 (s), 1292 (s), 1263 (s), 1201 (s), 1147 (s), 1095 (vs, v br), 1040 (s), 917 (s), 561 (s), 519 (s), 470 (s) cm^{-1}; XRD d = 12.9 Å; ^{13}C CP MAS NMR δ(COOH) 180.9 ppm, $\delta(CH_2)$ 28.0 ppm (v br); ^{31}P MAS NMR δ 12.4 ppm; TGA room temperature to 200 °C, 0%, 200–450 °C, –21.7%, 450–1150 °C, –11.2%.

Synthesis of $Zr(O_3PCH_2CH_2COO^-NH_4^+)_2$, 2. Anhydrous ammonia (National-Bower) was passed through a flask containing 5 g of **1** for 24 h. **2**: IR (KBr) 3600–2500 (s, v br), 1550 (s, br), 1421 (s), 1404 (s), 1107 (s), 1040 (vs, v br) cm^{-1}; XRD d = 15.3 Å; ^{13}C CP MAS NMR $\delta(COO^-)$ 183.0 ppm, $\delta(CH_2)$ 33.0 ppm (v br); ^{31}P MAS NMR δ 8.0 ppm; TGA room temperature to 200 °C, –7.6%, 200–700 °C, –21.3%.

General Procedure for the Synthesis of $Zr(O_3PCH_2CH_2COO^-NH_3^+C_nH_{2n+1})_2$, 2(*n*). *n*-Alkylamines (C_3–C_{16}) were intercalated into **1** from dilute methanol or aqueous solutions (0.2 M) according to published procedures.[18] Longer chain (C_{10}–C_{16}) ammonium intercalates of **1** were also prepared by ion-exchange reactions from the hexylammonium intercalate by heating a mixture of 0.3 g of **2(6)**, 15 mL of absolute ethanol, and 0.2 g of alkylamine at 55 °C for 1 week in a sealed 25-mL test tube. The solid product was collected by filtration, washed with ethanol and acetone, and dried at room temperature to a constant weight. **2(6)**: IR (KBr) 3600–2500 (m, v br), 2959 (s), 2930 (s), 2872 (s), 2859 (s), 1635 (m), 1560 (s), 1422 (m), 1402 (m), 1105 (s), 1030 (vs, br) cm^{-1}; XRD d = 28.0 Å; TGA room temperature to 220 °C, –22.7%, 220–450 °C, –10.9%, 450–700 °C, –21.3%; ^{13}C CP MAS NMR δ(COO) 181.8 ppm, $\delta(CH_2)$ 41.3, 33.0, 31.6, 28.7, 24.0 ppm, $\delta(CH_3)$ 14.7 ppm; ^{31}P MAS NMR δ 8.2 ppm.

Synthesis of $Zr(O_3PCH_2CH_2COCl)_2$, 3. The layered acyl chloride, **3**, was prepared as described in a previous publication.[19] **3**: IR (KBr) 2962 (w), 2932 (w), 1793 (s), 1411 (m), 1231 (s), 1060 (vs, v br), 951 (s), 507 (s) cm^{-1}; XRD d = 13.5 Å; ^{13}C CP MAS NMR δ(COCl) 173.7 ppm, $\delta(CH_2)$ = 0 (br), 25 (v br), 42 ppm (br); ^{31}P MAS NMR δ 5.5 ppm.

Synthesis of $Zr(O_3PCH_2CH_2CONH_2)_2$, 4. Anhydrous ammonia was passed through a flask containing 1 g of **3** for 10 days. The product was washed with water and dried to a constant weight at 100 °C. **4**: IR (KBr) 3224 (s, br), 3203 (s, br), 1659 (s), 1418 (m), 1258 (m), 1222 (m), 1050 (vs, v br), 547 (s) cm^{-1}; XRD d = 13.8 Å.

General Procedure for the Synthesis of $Zr(O_3PCH_2CH_2CONHC_nH_{2n+1})_2$, 4(*n*). The appropriate *n*-alkylamine (25 g) was added to 1 g of **3**. The mixture was warmed to 80 °C, where it was stirred for 2 weeks under a dry nitrogen atmosphere. The solid product was collected on a fritted glass filter, washed with water and acetone, and dried to a constant weight at 100 °C. **4(6)**: IR (KBr) 3325 (s, br), 3081 (m, br), 2959 (s), 2928 (s), 2859 (s), 1645 (s), 1549 (s), 1261 (m), 1103 (vs), 1050 (vs, v br), 557 (m) cm^{-1}; XRD d = 27.0 Å; TGA room temperature to 260 °C, –3.0%, 250–390 °C, –20.5%, 390–700 °C, –20.8%.

Synthesis of $Zr(O_3PCH_2CH_2CONHC_{12}H_{24}NHCOCH_2CH_2PO_3)$. 1,12-Diaminododecane (8.25 g) was added to 0.5 g of **3**. The mixture was stirred at 80 °C for 8 days under an argon atmosphere. The solid product was collected on a fritted glass filter, washed with water, acetone, and ethanol, and dried to a constant weight at 100 °C. IR (KBr) 3338 (s, br), 2920 (vs), 2851 (vs), 1647 (s), 1577 (s), 1489 (s), 1471 (s), 1392 (s), 1321 (s), 1099 (s), 1034 (vs, br) cm^{-1}; XRD d = 27.4 Å.

General Procedure for the Synthesis of $Zr(O_3PCH_2CH_2COOC_nH_{2n+1})_2$, 5(*n*). The appropriate *n*-alkyl alcohol (25 g) was added to 1 g of **3**. The mixture was warmed to 80 °C, where it was stirred for 2 weeks under a dry nitrogen atmosphere. The solid product was collected on a fritted glass filtered, washed with water and acetone, and dried to a constant weight at 100 °C. **5(6)**: IR (KBr) 2960 (s), 2920 (s), 2870 (s), 2860 (s), 1737 (s), 1248 (s), 1177 (m), 1104 (vs), 1045 (vs, v br), 553 (m) cm^{-1}; XRD d = 25.6 Å; TGA: room temperature to 200 °C, –0.0%, 200–700 °C, –52.4%.

Synthesis of $Zr(O_3PCH_2CH_2C(O)OCH_2CH_2CH_2P_3O)\cdot x Bu_3SnCl$, 6. Bu_3SnH (10 mL) was added to a flask containing 1 g of **3** under Ar; the mixture was stirred for 2 weeks at 60 °C under an Ar purge. The solid product was collected on a glass frit, washed with water and acetone, and dried. The product was

(16) (a) Troup, J. M.; Clearfield, A. *Inorg. Chem.* **1977**, *16*, 3311–3314. (b) Albertsson, J.; Oskarsson, Å .; Tellgren, R.; Thomas, J. O. *J. Phys. Chem.* **1977**, *81*, 1574–1578.

(17) Környei, J.; Szirtes, L. *J. Radio. Nucl. Chem.* **1984**, *83/2*, 257–260.

(18) Környei, J.; Szirtes, L.; Constantino, U. *J. Radioanal. Nucl. Chem.* **1985**, *89/2*, 331–338.

(19) Burwell, D. A.; Thompson, M. E. *Chem. Mater.* **1991**, *3*, 14–17.

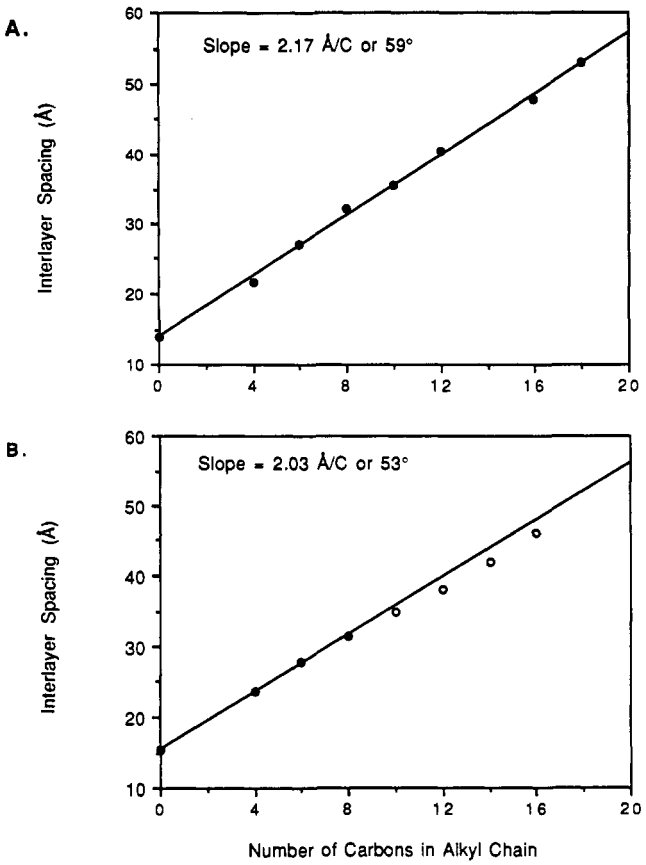

Figure 3. Interlayer spacings of (A) **4(*n*)** and (B) **2(*n*)** versus guest alkyl chain length. The standard deviation for each *d* spacing is no greater than 0.7 Å; filled circles denote single-phase products; open circles denote mixed-phase products.

washed further in refluxing toluene, collected on a frit, washed with acetone, and dried at 100 °C. **6**: IR (KBr) 3600–3200 (m, v br), 2960 (m), 2920 (m), 2870 (w), 2860 (w), 1740 (s), 1254 (s), 1038 (vs, v br), 550 (m) cm^{-1}; XRD *d* = 24.7–15.1 Å (depending on amount of Bu_3SnCl); ^{13}C CP MAS NMR of *d* = 15.1 Å phase δ(COO) 173.6 ppm, δ(CH_2, CH_3) 53.4, 28.6, 23.5, 22.3, 16.9, 14.6, −2.0 ppm.

Results and Discussion

The primary goal of this work was to develop new reactions that promote intercalation. A secondary goal was to use these reactions to prepare novel layered organic–inorganic materials and to compare the physical and chemical properties of these materials to those of more traditional intercalation compounds. The layered host chosen for our initial work was the acyl chloride derivative, **3**, of a well-characterized zirconium phosphonate, **1**. The synthesis of **3** from **1** has been described in a previous communication.[19]

With the above objectives in mind, our first reaction for **3** involved treatment with *n*-alkylamines. The product of this reaction should be a layered secondary amide. In contrast to amine intercalation of **1**, the driving force for this intercalation reaction is the formation of a covalent host–guest bond. Amides are ideal for judging any stability enhancement resulting from the covalent linkage since their physical, chemical, and thermal properties can be compared to those of the equivalent alkylammonium intercalation compounds of **1**.

To augment the published data on alkylamine intercalation compounds of **1**,[5a,18] *n*-alkylamine intercalates with carbon chain length C_3–C_{16} were prepared and characterized in this laboratory. *n*-Alkylamines were intercalated into **1** from dilute (0.2 M) methanol or aqueous solutions. The longer chain (C_{10}–C_{16}) ammonium intercalates of **1** were also prepared by ion-exchange reactions from the hexylammonium intercalate, **2(6)**. **1** did not intercalate *n*-octadecylamine under any of these conditions or when contacted with the neat liquid amine at 80 °C.

Only ammonia and unbranched primary *n*-alkylamines fully intercalate into α-ZrP or **1** to form stoichiometric ammonium salts. Branched primary amines and secondary and tertiary amines are tyically too bulky to form stoichiometric salts with these hosts, as they cover adjacent acid sites on the host lamellae. In general, only guest molecules with cross-sectional areas less than the free surface area of each phosphate or phosphonate site (ca. 24 $Å^2$)[16a,20] will form stoichiometric intercalation compounds. For example, we have found that $(C_2H_5)_2CHNH_2$ reacts with approximately 75% of the carboxylic acid sites in **1** (based on IR and TGA to give $Zr(O_3PCH_2CH_2COO^-(C_2H_5)_2CHNH_3^+)_{1.5}(O_3PCH_2CH_2COOH)_{0.5}$ (*d* = 22.0 Å).

3 appears to intercalate guest molecules in a shape-selective manner similar to that of **1**. Thus, ammonia and unbranched primary amines fully intercalate, but branched primary and secondary amines do not. This result is not surprising, given that **1** and **3** have identical surface constraints. Secondary amines, **4(*n*)**, were prepared by contacting **3** with neat liquid *n*-alkylamines under a nitrogen atmosphere, eq 5. The primary amide, **4**, was prepared

$$Zr(O_3PCH_2CH_2COCl)_2 \xrightarrow{RNH_2} Zr(O_3PCH_2CH_2CONRH)_2 + HCl \quad (5)$$

$$Zr(O_3PCH_2CH_2COCl)_2 \xrightarrow{NH_3(g)} Zr(O_3PCH_2CH_2CONH_2)_2 + HCl \quad (6)$$

by treating **3** with anhydrous ammonia, eq 6. Interestingly, $(C_2H_5)_2CHNH_2$ intercalates to the same extent (75%) in **3** (based on IR and TGA) as in **1** to yield $Zr(O_3PCH_2CH_2C(O)NHCH(C_2H_5)_2)_{1.5}(O_3PCH_2CH_2COOH)_{0.5}$ (*d* = 21.2 Å).

Powder XRD indicates that the layered structure of **1** is maintained upon conversion to **4** and **4(*n*)**. The diffraction patterns of the amides generally exhibit at least three orders of 00*l* reflections. The reflections are of comparable intensity to, yet narrower than, those of **3**. The interlayer spaces of the amides increase predictably with increasing alkyl chain length. Table I summarizes the interlayer spacings of all compounds prepared in this work. Figure 3 contains plots of the interlayer spacings of amide (A) and ammonium (B) intercalation compounds versus the number of carbons in the alkyl chain of the guest (N_C). In these plots, the interlayer spacings for N_C = 0 are those of the primary amide, **4**, and the NH_4^+ salt, **2**, respectively. The steady increase in interlayer spacings of the amides at a constant slope of 2.17 Å/CH_2 indicates that the nitrogen-bound alkyl chains are tilted at an angle of 59° with respect to the zirconium phosphonate layers or 31° from the bilayer normal. This calculation assumes that the guest molecules intercalate to form a bilayer of fully extended (i.e., all-trans) alkyl chains. On the basis of a typical methylene repeat distance of 1.27 Å/CH_2 for an all-trans polymethylene chain, the interlayer spacing of a bilayer with fully extended alkyl chains perpendicular to the inorganic layers would be expected to increase by 2 times 1.27 Å/CH_2, or 2.54 Å/CH_2. The tilt angle is taken as the arcsin of the ratio of the observed slope to 2.54 Å/CH_2. Thus, an observed slope of 2.17 Å/CH_2 yields a tilt angle

(20) Alberti, G.; Constantino, U.; Giovagnotti, M. L. L. *J. Inorg. Nucl. Chem.* **1979**, *41*, 643–647.

Table I. Interlayer Spacings of Compounds Prepared in This Study

no.	compound	interlayer dist, Å
1	$Zr(O_3PCH_2CH_2COOH)_2$	12.9
2	$Zr(O_3PCH_2CH_2COO^-NH_4^+)_2$	15.3
2(*n*)	$Zr(O_3PCH_2CH_2COO^-C_nH_{2n+1}NH_3^+)_2$	
2(3)	$n = 3$	22.6
2(4)	$n = 4$	23.6
2(6)	$n = 6$	28.0
2(8)	$n = 8$	32.3
2(10)	$n = 10$	35.7
2(12)	$n = 12$	38.0
2(14)	$n = 14$	42.0
2(16)	$n = 16$	46.0
3	$Zr(O_3PCH_2CH_2COCl)_2$	13.5
4	$Zr(O_3PCH_2CH_2CONH_2)_2$	13.8
4(*n*)	$Zr(O_3PCH_2CH_2CONHC_nH_{2n+1})_2$	
4(4)	$n = 4$	21.8
4(6)	$n = 6$	27.0
4(8)	$n = 8$	32.1
4(10)	$n = 10$	35.6
4(12)	$n = 12$	40.1
4(16)	$n = 16$	48.0
4(18)	$n = 18$	53.0
5(*n*)	$Zr(O_3PCH_2CH_2COOC_nH_{2n+1})_2$	
5(2)	$n = 2$	16.5
5(4)	$n = 4$	20.5
5(6)	$n = 6$	25.6
6	$Zr(O_3PCH_2CH_2COOCH_2CH_2CH_2PO_3)\cdot xBu_3SnCl$	24.7–15.1
	$Zr(O_3PCH_2CH_2CONHC_{12}H_{23}NHCOCH_2CH_2PO_3)$	27.4

of sin^{-1} (2.17/2.54), or 59°. The good linear curve fit of the data points in Figure 3A suggests that the amide bonding geometry remains fixed regardless of alkyl chain length.

In contrast, *n*-alkylamines of different length do not react so uniformly with 1. We have found that *n*-alkylamines with $3 \leq N_C \leq 8$ readily intercalate into 1 to form single-phase, stoichiometric compounds. However, *n*-alkylamines with $N_C > 8$ form mixtures of phases with 1, even when prepared at higher temperatures and concentrations and with much longer contact times. Furthermore, the interlayer spacing of the largest *d*-spaced phase in these mixtures is always less than that expected if the guest formed a bilayer with fully extended alkyl chains tilted at 59°. These results are depicted graphically in Figure 3B. Here, the filled circles represent well-characterized, single-phase amine intercalation compounds ($N_C \leq 8$), and the open circles show the *d* spacings of the largest *d*-spaced phase observed in a mixed-phase product for a given amine ($N_C > 8$). It is clear that the slope of the curve-fit changes distinctly at about $N_C = C_8$ and that both slopes are fairly constant. For $N_C < C_8$, the slope is 2.03 Å/CH_2, which translates to a 53° tilt angle. For $N_C > 8$, the slope of the curve fit (not shown for the sake of clarity) is 1.85 Å/CH_2—indicating a 47° tilt angle. The method of preparation of the longer chain ammonium intercalates did not affect their interlayer spacings. Long-chain amines ($N_C > 8$) intercalated directly into 1 and ion-exchanged for the shorter hexylammonium ion guest in **2(6)** gave products with identical interlayer spacings for a given amine.

The 59° and 53° tilt angles of amide and ammonium intercalates of 1, respectively, agree reasonably well with that reported by Környei et al.[18] for *n*-alkylammonium intercalates of 1. They report a 60° tilt angle based on a slope of 2.2 Å/CH_2 for alkylamine guests with $4 \leq N_C \leq 10$. They also report an interlayer spacing for the *n*-dodecylammonium intercalate that is smaller than expected based on a constant slope of 2.2 Å/CH_2. In addition, the 53° tilt angle we've found for alkylammonium intercalates of 1 is close to the angle found for alkylammonium intercalates of α-ZrP (which equals either 56° for N_C = even numbers[4a] or 52° for N_C = even and odd numbers[21]). In α-ZrP, the tilt angle is rationalized in terms of an all-trans polymethylene chain with an initial nitrogen–carbon bond perpendicular to the phosphate layers. This arrangement allows for maximum hydrogen bonding to the trigonal array of oxygen anions on the α-ZrP layer surfaces.

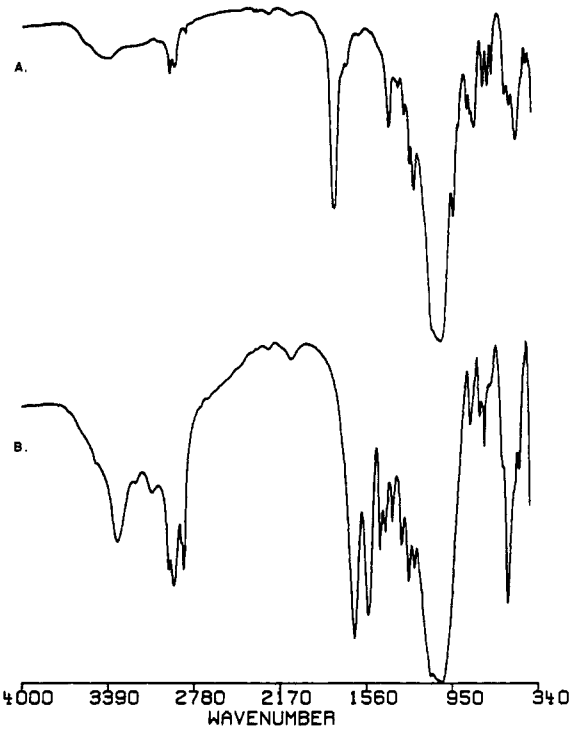

Figure 4. FTIR spectra of (A) 3 and (B) 4(8).

IR spectra of 4(*n*) are consistent with quantitative conversion of 3 and suggest a trans hydrogen-bonding geometry (Figure 4). All secondary amides prepared in this study have essentially identical IR spectra. Absorptions for amide I at 1646, amide II at 1548, and N–H stretches at ca. 3320 and 3080 cm^{-1} are exhibited. The range in absorption frequency for the amide I and amide II bands is less than 2 cm^{-1}. The relatively low frequency absorption for the amide I (ν_{CO}) band indicates that strong hydrogen bonding is present. The amide II band is due to the interaction between N–H bending and C–N stretching frequencies and requires a trans geometry. Together these absorptions suggest that *intralayer* hydrogen bonding is occurring—possibly as shown in Figure 5. Compound 4 exhibits characteristic primary amide bands in the IR at 3224 ($\nu_{as(NH)}$), 3203 ($\nu_{s(NH)}$), 1659 (ν_{CO}), and 1418 cm^{-1} (ν_{CN}). The amide II band appears as a low-energy shoulder on the amide I absorption.

^{13}C CP MAS NMR spectra of the layered secondary amides confirm that the conversion of 3 to 4(*n*) is quantitative. The carbonyl carbon resonance of 3 at 173.7 ppm is replaced by a very broad resonance at ca. 182 ppm in the spectrum of 4. The intensity of the 182 ppm peak is drastically reduced relative to 1 and 3 due to coupling to the adjacent quadrupolar ^{14}N nucleus. This is seen clearly in the spectra of 1 and 4(18) (Figure 6). The sharp, intense resonances of the carbon nuclei in the N-bound alkyl chain are superimposed on the broad resonances of the P- and C(O)-bound methylene carbons. The methylene carbons between the phosphorus and carbonyl group give very broad signals which are not effectively averaged by magic angle sample spinning. We believe the signal

(21) Tindwa, R. M.; Ellis, D. K.; Peng, G.; Clearfield, A. *J. Chem. Soc., Faraday Trans. 1* **1985**, *81*, 545–552.

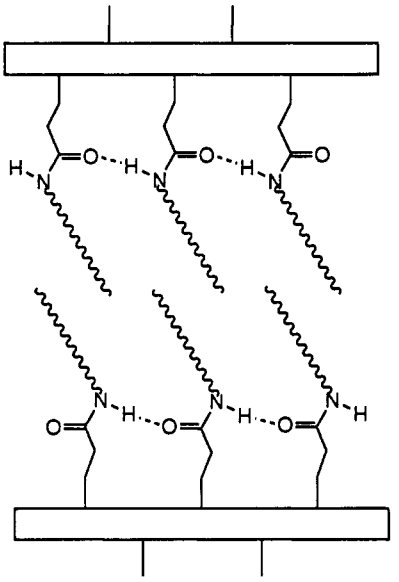

Figure 5. Schematic drawing of proposed intralayer hydrogen bonding in **4(*n*)**.

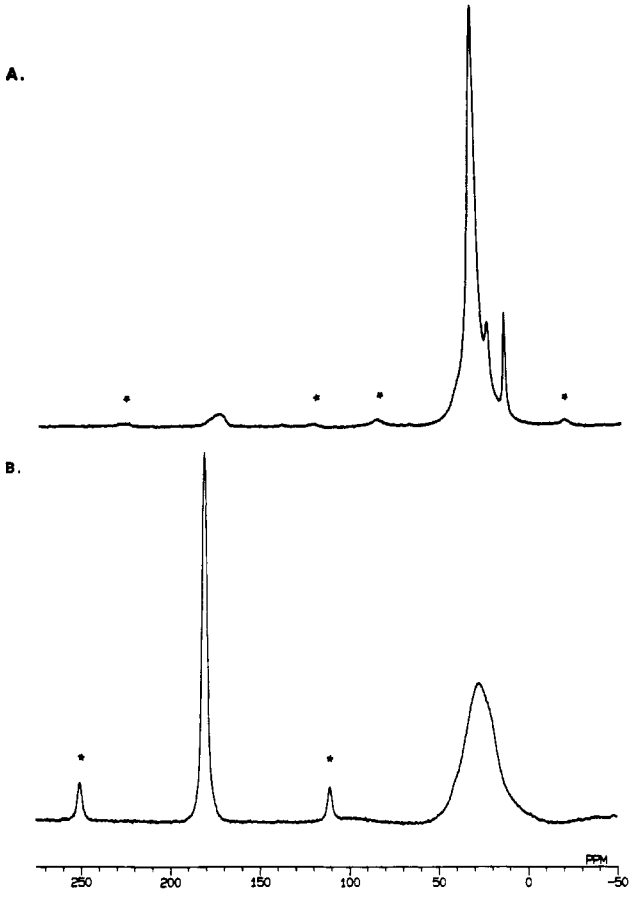

Figure 6. 67.9-MHz ^{13}C CP MAS NMR spectra of (A) **4(18)** and (B) **1**. The spectrum of **4(18)** was obtained with a 5.2-μs 90° pulse, 1500-μs mix time, and 2.0-s recycle delay. The spectrrum of **1** was obtained with a 7.0-μs 90° pulse, 1500-μs mix time, and 2.0-s recycle delay. Asterisks denote spinning sidebands.

broadening is due to a dispersion of local electronic environments for the methylenes, and investigations are underway to confirm such.

The bulk thermal stability of the secondary amide intercalates is significantly enhanced relative to the alkylammonium intercalates. Figure 7 shows TGA plots of **4(6)** (upper curve) and **2(6)** (middle curve) obtained with the

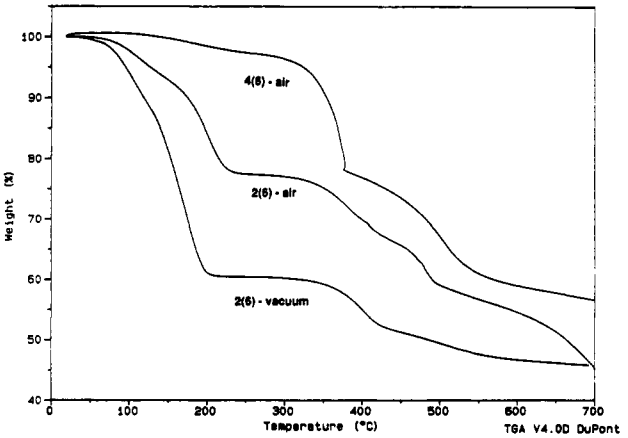

Figure 7. Thermogravimetric analyses of **4(6)** and **2(6)** under air and **2(6)** under vacuum.

samples exposed to an air atmosphere. The plots suggest that the two types of intercalation compounds may follow different decomposition pathways. Upon heating, it appears that **2(6)** decomposes by a three-step process that starts with the deintercalation and evaporation of the hexylamine guest at relatively low temperature (<220 °C). This is likely followed by pyrolysis of the remaining organics at intermediate temperature (400 °C) and condensation of the phosphonate groups at high temperature to yield crystalline ZrP_2O_7. In contrast, the organic portion of **4(6)** appears to remain essentially intact to ca. 350 °C, at which point it pyrolyzes very rapidly. Above ca. 400 °C, **4(6)** behaves similarly to **2(6)**—ultimately forming ZrP_2O_7.

Unfortunately, the TGA curves of both of these materials are complicated by the incomplete loss of interlayer carbon during decomposition. That is, some organic pyrolysis products become trapped in the inorganic matrix and are only slowly lost during the phosphonate condensation step. Thus, prolonged exposure (>30 min) to air at ca. 1000 °C is typically required to form crystalline ZrP_2O_7. This phenomenon, which is common to all layered zirconium phosphonates we have studied, often results in gradual weight losses that sometimes cannot be unambiguously assigned. The problem is alleviated to some degree for the electrostatic intercalation compounds by running the analyses under vacuum instead of air. Under vacuum the alkylamine guest molecules tend to deintercalate more cleanly and at a lower temperature, as evidenced by the TGA of **2(6)** run under vacuum (Figure 7, lower curve). On the other hand, the temperature at the onset of weight loss and the percent weight loss in the TGAs of **4(*n*)** run under vacuum are unchanged relative to those run in air.

In the TGA of **2(6)** in air, the onset of the first weight transition—which totals 22.7%—occurs below 100 °C and is complete by 220 °C. The midpoint temperature (i.e., the temperature at the inflection point of the weight transition) of the steeper part of the weight loss is 203 °C. Again, this weight loss is due to the partial deintercalation and evaporation of the hexylamine guest (bp ≈ 131 °C). Deintercalation of all hexylamine guest molecules would result in a 33.9% weight loss. The more gradual 32.2% weight loss between 250 and 700 °C combines the loss of the remaining organics and condensation of the phosphonates. When run under vacuum, the TGA of **2(6)** exhibits two well-resolved transitions. The first transition is similar in shape to the transition seen in the TGA in air; however, the weight loss (39.8%) is substantially greater and the midpoint temperature (170 °C) is lower. The second weight loss (14.3%) under vacuum occurs at a

midpoint temperature of 400 °C. This latter transition looks very much like the major transition observed for 1 run under vacuum (21.7%, 425 °C). In fact, a transition identical with the 21.7% weight loss of 1 would correspond to a 14.4% loss in **2(6)**. These data indicate that the hexylamine guest fully deintercalates below 200 °C, leaving the regenerated acid host to decompose at a higher temperature.

In contrast to the TGA curve of **2(6)**, that of **4(6)** shows only a 3.0% weight loss between room temperature and 260 °C. This loss may be due to excess hexylamine or adsorbed water. The first major transition occurs at a midpoint temperature of 370 °C and accounts for 20.5% of the total weight. As mentioned above, this loss is due to pyrolysis of the organic pendant group. An additional 20.8% weight is lost between 390 and 700 °C as trapped carbon is liberated and phosphonate groups condense. The total weight lost in conversion to ZrP_2O_7 was 53.2%; the theoretical weight loss is 52.8%.

C, H, N analysis by flash combustion was of limited use in confirming exact stoichiometries of **4(*n*)**. The experimentally determined values for **4(6)** were 33.7% C, 5.9% H, and 5.0% N; the theoretical values are 38.5% C, 6.5% H, and 5.0% N. Again, we believe the low carbon value is most likely due to trapping of organic pyrolysis products in the inorganic matrix. With the short burn time used for flash combustion analysis (i.e., < 30 s), trapping of carbonaceous material leads to highly variable compositional data. Other investigators have previously noted this problem for layered metal phosphonates.[22] For this reason, we regard our thermal analysis data as a more reliable measure of composition when the TGA is run under an oxygen atmosphere (vide supra).

The chemical stability of the secondary amides is also enhanced relative to the alkylammmonium intercalation compounds. For example, **4(12)** stirred in 3 M HCl at 60 °C for 5 days showed less than 10% hydrolysis as determined by IR and powder XRD. The interlayer spacing of the partially hydrolyzed product was 38 Å—a decrease of only 2 Å from the starting decylamide. On the other hand, **2(12)** was cleanly converted to **1** in less than 3 h under the same conditions.

Layer-bridging diamides can be formed by intercalation of alkyldiamines into **3**. For example, the product of the reaction between **3** and 1,12-diaminododecane was a layered solid with an interlayer spacing of 27.4 Å and IR spectrum very similar to those of **4(*n*)**. The 27.4-Å interlayer spacing is consistent with a diamide monolayer that bridges adjacent layers. The fact that the interlayer spacing is larger than that of **4(6)** (d = 27.0 Å) indicates that the alkyl chains in the diamide monolayer are tilted at a greater angle from the inorganic layers than those in monoamide bilayers.

Ester derivatives, **5(*n*)**, were also prepared from **3** in quantitative yields. The synthesis was essentially identical with that of secondary amides—that is, contact the solid acyl chloride with neat liquid n-alkyl alcohols under a dry nitrogen atmosphere (eq 7). The three ester compounds

$$Zr(O_3PCH_2CH_2COCl)_2 \xrightarrow{ROH} Zr(O_3PCH_2CH_2COOR)_2 + HCl \quad (7)$$

prepared (R = C_2H_5, C_4H_9, and C_6H_{13}) exhibited very similar IR spectra, with prominent ester absorptions of ν_{CO} at 1737, ν_{COC} at 1248, and δ_{OCO} at 550 cm^{-1}. The frequency of the C=O and C–O–C stretches varied by less than 2 cm^{-1} in these compounds. The carbonyl resonance of **5(4)** appears at 173.9 ppm in the ^{13}C CP MAS NMR spectrum. Methylene resonances are found at 65.6, 31.4, and 19.9 ppm, and the terminal methyl peak appears at 14.3 ppm.

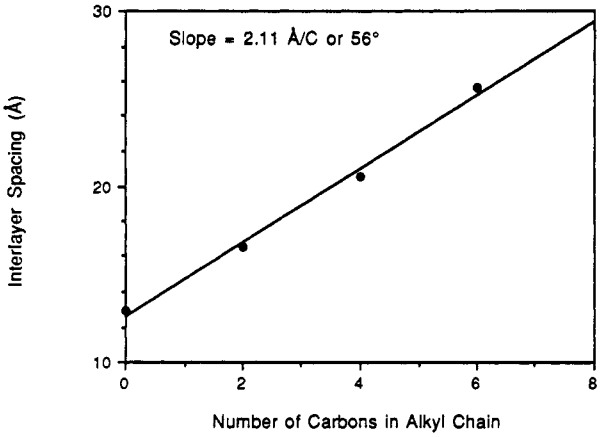

Figure 8. Interlayer spacings of **5(*n*)** versus guest alkyl chain length.

The interlayer spacings of the ester derivatives are reported in Table I and are plotted versus N_C in Figure 8. In this graph the data point at N_C = 0 is the interlayer spacing of 1. The curve fit yielded a slope of 2.11 Å/CH_2, corresponding to a 56° tilt angle with respect to the inorganic layers. Again, this angle is nearly identical with that for alkylamine intercalates of 1 and α-ZrP. The thermograms of these materials are relatively easy to interpret. For example, the TGA of **5(6)** obtained in air exhibits a single, sharp weight transition of 52.4% at a midpoint temperature of 365 °C. The theoretical weight loss for the conversion of this compound to ZrP_2O_7 is 53.0%. It is interesting that trapping of interlayer carbon is not observed during thermal analysis of ester derivatives.

A different kind of intercalation reaction was observed when **3** was treated with Bu_3SnH. The expected product was the layered aldehyde derivative (eq 8); however, it

$$Zr(O_3PCH_2CH_2COCl)_2 \xrightarrow{Bu_3SnH} Zr(O_3PCH_2CH_2CHO)_2 + Bu_3SnCl \quad (8)$$

$$Zr(O_3PCH_2CH_2COCl)_2 \xrightarrow{Bu_3SnH} Zr(O_3PCH_2CH_2C(O)OCH_2CH_2CH_2PO_3) + Bu_3SnCl \quad (9)$$

appears that an *intralayer* ester derivative, **6**, was produced instead (eq 9). The ester is likely formed by the mechanism proposed by Lusztyk et al. for the equivalent solution chemistry.[23] According to this mechanism, the initial products of the reaction between **3** and Bu_3SnH would be aldehyde and Bu_3SnCl. However, before all the acyl chloride has been converted to aldehyde, a second equivalent of Bu_3SnH reacts with the aldehyde to form an alkoxytin species, possibly $-PCH_2CH_2CH_2OSnBu_3$. The alkoxytin species then apparently reacts with an adjacent acyl chloride to form the intralayer ester.

The IR spectrum of **6** is nearly identical with those of **5(*n*)**. Characteristic ester absorptions at 1740 (ν_{CO}), 1254 (ν_{COC}), and 550 (δ_{OCO}) cm^{-1} are all within 4 cm^{-1} of those exhibited in **5(*n*)**. The ^{13}C CP MAS NMR spectrum of **6** is also quite similar to those of **5(*n*)**. The spectrum showed a carbonyl carbon resonance at 173.6 ppm and an oxygen-bound methylene resonance at 53.4 ppm. A peak at 179.3 ppm suggests that some carboxylic acid was re-

(22) Alberti, G.; Constantino, U.; Kornyei, J.; Giovagnotti, L. *React. Polym.* **1985**, *4*, 1–10.

(23) Lusztyk, J.; Lusztyk, E.; Maillard, B.; Ingold, K. U. *J. Am. Chem. Soc.* **1984**, *106*, 2923–2931.

generated. However, IR data suggest that the acid comprises less than 10% of the product. The NMR spectrum also indicated the presence of trapped Bu_3SnCl. This fact accounts for the anomalously large and variable interlayer spacing found for **6**. Powder XRD patterns showed three orders of 00*l* reflections with an interlayer spacing ranging from 24.7 to 15.1 Å, depending upon the amount of Bu_3SnCl trapped between the layers. Bu_3SnCl can be partially removed by washing the solid in refluxing toluene; however, even the 15.1-Å phase contains a significant amount of Bu_3SnCl. The appearance of two weight losses totalling ca. 45% in the TGA of **6** (15.1-Å phase) provided additional evidence that Bu_3SnCl was present in the compound. The first weight loss of 25.1% occurred at a midpoint temperature of 390 °C; the second loss of 20.1% occurred at 1025 °C. If Bu_3SnCl had been removed during the reaction or subsequent washing, the expected total weight loss for the ester would be ca. 27%.

Much of the above chemistry has also been carried out with other members of the layered carboxylic acid zirconium phosphonate family—$Zr(O_3P(CH_2)_nCOOH)_2$. To date, we have been unable to prepare pure phases of $Zr(O_3PCH_2COCl)_2$ and $Zr(O_3P(CH_2)_3COCl)_2$. It may be that the reactivity of $Zr(O_3P(CH_2)_nCOOH)_2$ is related to structural and/or electronic changes in the carboxylic acid region. For example, the orientation of the pendant acid group relative to the inorganic layers is expected to change as a function of the number of methylene spacers (n = odd or even number) between phosphorus and the acid group. We are currently addressing this structure–reactivity question through more detailed intercalation studies and with multinuclear NMR spectroscopy.

Conclusion

By and large the intercalation of organic guests into inorganic hosts have been promoted by only three types of reactions: acid/base, ion exchange, and redox. By use of functionalized group 4 metal phosphonates it is possible to employ other reactions, common in organic chemistry, to promote intercalation. Here we reported the synthesis of amides and esters from an acid chloride derivative. These materials are well ordered, thermally stable, and easily characterized. The wide range of functional groups available in these metal phosphonates suggests that our syntheses of amides and esters may be only the first examples of a large number of novel organic reactions that will promote the intercalation of organic molecules into layered inorganic solids.

Acknowledgment. Acknowledgment is made to the donors of the Petroleum Research Foundation, administered by the American Chemical Society, and to the Air Force Office of Scientific Research (AFOSR-90-0122) for the support of this project.

Fourier Transform Infrared Spectroscopic Study of Predeposition Reactions in Metalloorganic Chemical Vapor Deposition of Gallium Nitride

B. S. Sywe, J. R. Schlup, and J. H. Edgar*

Department of Chemical Engineering, Durland Hall, Kansas State University, Manhattan, Kansas 66506-5102

Received February 12, 1991. Revised Manuscript Received May 10, 1991

The predeposition reactions that occur during metalloorganic chemical vapor deposition (MOCVD) of gallium nitride (GaN) were studied with Fourier transform infrared (FTIR) spectroscopy. The reactants studied included trimethylgallium (TMGa), ammonia (NH_3), and nitrogen trifluoride (NF_3). At room temperature, the predeposition reaction between TMGa and NH_3 went to completion immediately after mixing. The resulting adduct, TMGa:NH_3, was easily observed in the gas phase via FTIR spectroscopy. Assignments have been made to the IR absorption bands of gaseous TMGa:NH_3. At 150 °C, chemical equilibrium was reached between the gaseous adduct, TMGa:NH_3, and the reactants. The forward rate constant of this predeposition reaction is 5.89×10^{-3} (Torr s)$^{-1}$. No evidence of gas-phase adduct formation was observed when NF_3 was mixed with TMGa at room temperature and at 150 °C. This suggests a potential advantage of NF_3 over NH_3 as a nitrogen source in MOCVD of GaN.

Introduction

In the past two decades, metalloorganic chemical vapor deposition (MOCVD) has become one of the most widely used thin-film growth techniques for producing a complete range of III–V and II–VI compound semiconductor materials because of its technical simplicity and flexibility.[1-4] The MOCVD process is typically accomplished by the reaction of reactive metal–alkyls with a hydride of the nonmetal component. However, these precursors are very susceptible to forming adducts, even at room temperature, because metal–alkyls act as Lewis acids and the hydrides act as Lewis bases.[2] Thus, a difficulty commonly encountered in MOCVD processing of several compound semiconductors is the room-temperature predeposition of a nonvolatile adduct when the gaseous hydride is mixed with the metalloorganic vapor. Formation of nonvolatile adducts makes reliable transport of the reactants to the deposition zone difficult; thus precise control of both the

*To whom correspondence should be addressed.

(1) Leys, M. R. *Chemtronics* **1987**, *2*, 155.
(2) Ludowise, M. J. *J. Appl. Phys.* **1985**, *58*, R31.
(3) Razeghi, M. *The MOCVD Challenge*; Adam Hilger: Philadelphia, PA, 1989; Vol. 1, p 9.
(4) Stringfellow, G. B. *Organometallic Vapor-Phase Epitaxy: Theory and Practice*; Academic Press: San Diego, CA, 1989; p 6.

0897-4756/91/2803-0737$02.50/0